SUPPLEMENTARY METHODS

Density functional theory calculations

We use the generalised gradient approximation to density functional theory (DFT) proposed by Perdew, Burke, and Ernzerhof (PBE)[1] as is implemented in the VASP software package[2]. The "projector augmented wave" method is employed to represent the ionic cores[3], considering the following electrons as valence states: Ga's $4s$ and $4p$; P's $3s$ and $3p$; Zn's $3d$ and $4s$; and S's $3s$ and $3p$. Wave functions are represented in a plane-wave basis truncated at 500 eV. For integrations within the Brillouin zone (BZ) we employ Monkhorst–Pack $\mathbf{k}$–point grids with a density equivalent to $14 \times 14 \times 14$ in the unit cell. By using these parameters we obtain zero-temperature energies converged to within 0.5 meV per formula unit. Geometry relaxations are performed by using a conjugate–gradient algorithm that allows for cell volume and shape variations; the geometry relaxations are halted after the forces on the atoms fall below 0.01 eV·Å^{-1}. In order to reproduce site-occupancy disorder we adopt a 16–atom simulation cell constructed by replicating $2 \times 2 \times 2$ ($2 \times 2 \times 1$) times the elemental 2–atom (4–atom) zinc-blende (wurtzite) unit cell (see next section). We checked that the lattice parameters obtained with the PBE exchange-correlation potential are in good agreement with the observations; for instance, for bulk zinc-blende GaP and ZnS we estimate $a_0^{\rm PBE} = 5.52$ and 5.46 Å, respectively, compared with the experimental values $a_0^{\rm exp} = 5.45$ and 5.41 Å [4]. Nevertheless, PBE seriously underestimates the corresponding energy band gaps (as expected); for instance, for bulk zinc-blende GaP and ZnS we calculate $E_{\rm gap}^{\rm PBE} = 1.6$ and 2.1 eV, respectively, compared with the experimental values $E_{\rm gap}^{\rm exp} = 2.3$ and 3.5 eV[4,5]. In order to obtain accurate energy band gaps we employ the hybrid HSE06 functional[6], which is known to be appropriate for this purpose. In fact, we estimate $E_{\rm gap}^{\rm HSE06} = 2.3$ and 3.1 eV for bulk zinc-blende GaP and ZnS, respectively. Due to the high computational load associated with free-energy calculations (see below), here we employ the PBE functional for performing geometry relaxations and energy evaluations, and the hybrid HSE06 functional for estimating the resulting electronic features.

The calculation of phonon frequencies is performed with the small displacement method[7], in which the force-constant matrix is calculated in real-space by considering the proportionality between atomic displacements and forces when the former are sufficiently small[8]. After

the force-constant matrix is calculated, we apply a Fourier-transformation to obtain the phonon spectrum at any **q**-point. The impact of long-range interactions on the calculation of long-wavelength phonons has been disregarded because we are primarily interested in the estimation of quasi-harmonic free energies, and in such a context those effects are known to be secondary[9,10]. The quantities with respect to which our phonon calculations need to be converged are the size of the supercell, the size of the atomic displacements, and the numerical accuracy in sampling the BZ. We find the following settings to provide quasi–harmonic free energies converged to within 5 meV per formula unit: 128–atom supercells (generated by replicating $2\times2\times2$ the 16–atom unit cell mentioned above), atomic displacements of 0.02 Å, and q-point grids of $16\times16\times16$. The value of the phonon frequencies and quasi–harmonic free energies are obtained with the PHONOPY code[11]. In using this code we exploit the translational invariance of the system to impose that the three acoustic branches are exactly zero at Γ, and perform central differences in the atomic forces.

In order to estimate the positions relative to vacuum of the valence and conduction bands in $(GaP)_x(ZnS)_{1-x}$ solid solutions we employ the CRYSTAL09 code[12]. Previously published basis sets are used for the atoms[13–15] (i.e., $86-4111(d41)$ for Zn, $86-311(d)$ for S, and pseudopotentials for Ga and P) along with the hybrid B3PW method[16] with a 15% of Hartree–Fock exchange energy. The basis set parameters for the valence functions were re-optimized in order to reproduce as closely as possible the energy band gaps and lattice parameters of bulk zinc-blende GaP and ZnS (e.g., $E_{\rm gap}^{\rm B3PW}=2.6$ and 3.4 eV, respectively). Monkhorst–Pack **k**–point grids of at least $8\times8\times8$ are used, rendering total energies converged to within 1 meV per formula unit. In these calculations, the solid solution structures were fully relaxed, including both lattice parameters and atomic positions.

Tests on multi-configurational supercell calculations

Due to the huge computational expense associated with first-principles estimation of phonon excitations for a large number of configurations, we calculate $F_{\rm vib}$ just for the structure rendering the highest $\tilde{p}_m$ probability at room temperature. This choice has been justified in the main text (i.e., due to the highly peaked nature of the occurrence probability distributions in GaP–ZnS solid-solutions), however we performed a simple test to assess the effects of choosing a different configuration on the evaluation of $F_{\rm vib}$. Specifically, the vibrational

free energy of the most and least probable zinc-blende $(GaP)_{0.25}(ZnS)_{0.75}$ configurations at $T = 300$ K were calculated, with the finding that they differed by less than 10 meV per formula unit within the interval $300 \leq T \leq 1000$ K. Variations on the local degree of disorder in GaP–ZnS solid solutions, therefore, do not appear to lead to significant differences in the vibrational free energy features of the system. Based on this outcome, we may conclude that our approach for estimating vibrational free energy contributions, although it is not statistical in nature due to obvious computational limitations, provides reasonably accurate $F_{\rm vib}$ results (i.e., to within 10 meV/f.u.).

Concerning the numerical errors associated with finite-size effects in our multi-configurational supercell calculations, we carried out additional calculations in a 24–atom supercell to estimate the numerical uncertainties in our configurational mixing free-energy results. In particular, we calculated ΔF for a $x = 1/12$ composition in a 24–atom supercell and compared the results to those obtained via interpolation in a 16–atom supercell. At $T = 300$ K (1000 K), we compute a mixing free-energy (neglecting vibrational contributions) of 0.029 (0.011) eV/f.u. in the 24–atom supercell and of 0.039 (0.018) eV/f.u. in the 16–atom supercell. Consequently, we may conclude that the typical numerical uncertainty in our ΔF results is of the order of 10 meV per formula unit AB.

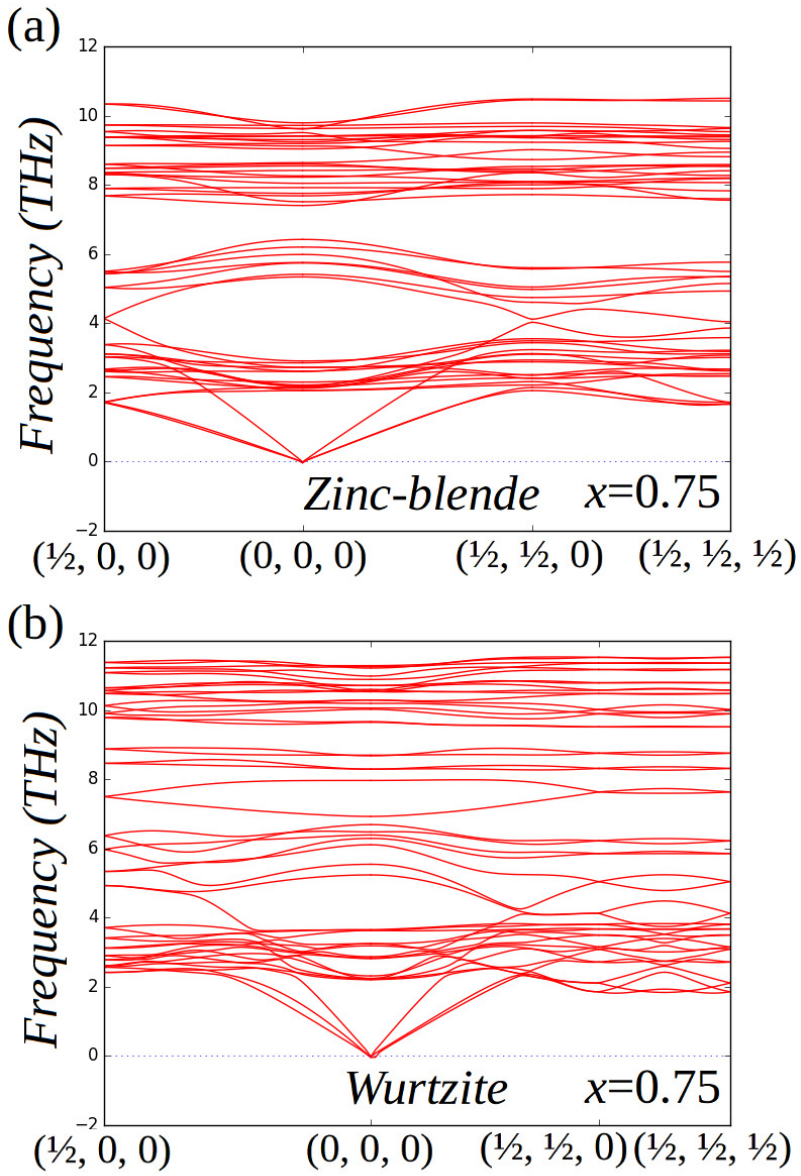

Supplementary Figure 1: Phonon spectra of $(GaP)_{0.75}(ZnS)_{0.25}$ solid solutions in the zinc-blende and wurtzite structures. Calculations are performed with the small-displacement method[7–10]. High-frequency lattice vibrations are more energetic in the wurtzite phase.

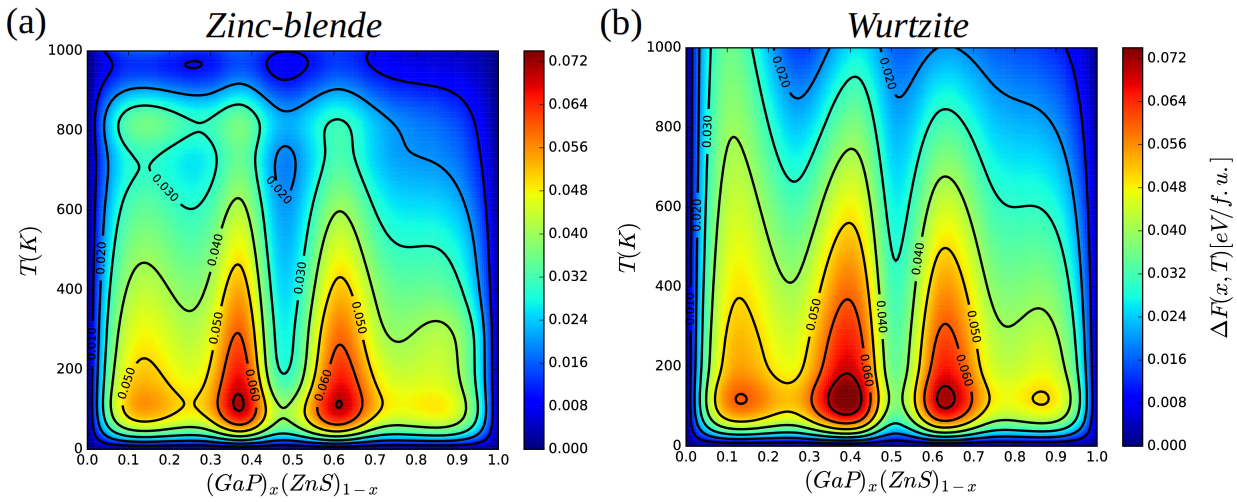

Supplementary Figure 2: Mixing free-energy of $(\mathrm{GaP})_x(\mathrm{ZnS})_{1-x}$ solid solutions as a function of temperature and composition, estimated without considering $T \to \infty$ corrections in the configurational free energy. (a) Zinc-blende and (b) wurtzite structures. Solid lines represent isovalue ΔF contours expressed in units of eV per formula unit. The conclusions presented in the main text, which are obtained after applying a correction term to the configurational free energies, are qualitatively equivalent to the ones deduced from this figure. Typical ΔF errors are estimated to be of the order of 10 meV per formula unit.

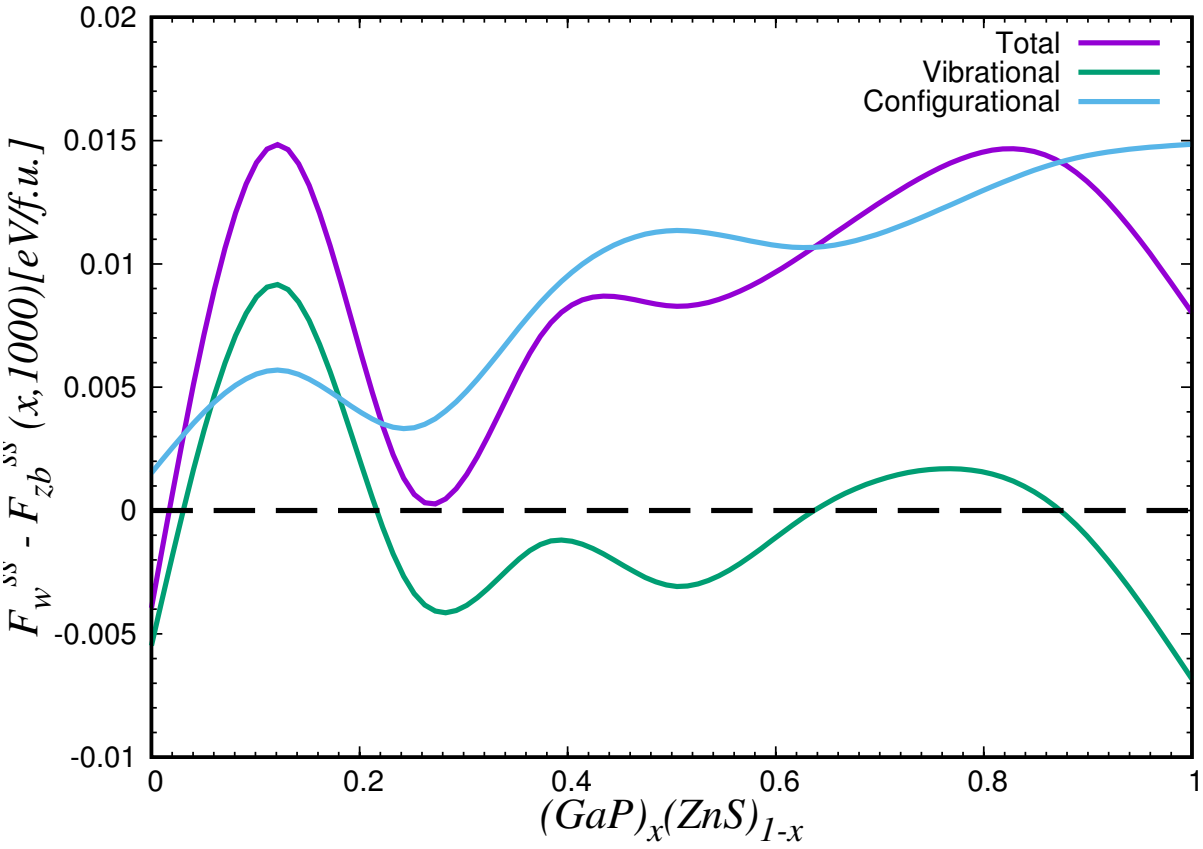

Supplementary Figure 3: Free–energy difference between polymorphs in $(GaP)_x(ZnS)_{1-x}$ solid solutions at $T = 1000$ K. Zinc-blende and wurtzite phases are represented as "zb" and "w", respectively. Configurational and vibrational contributions to the total free–energy difference are indicated.

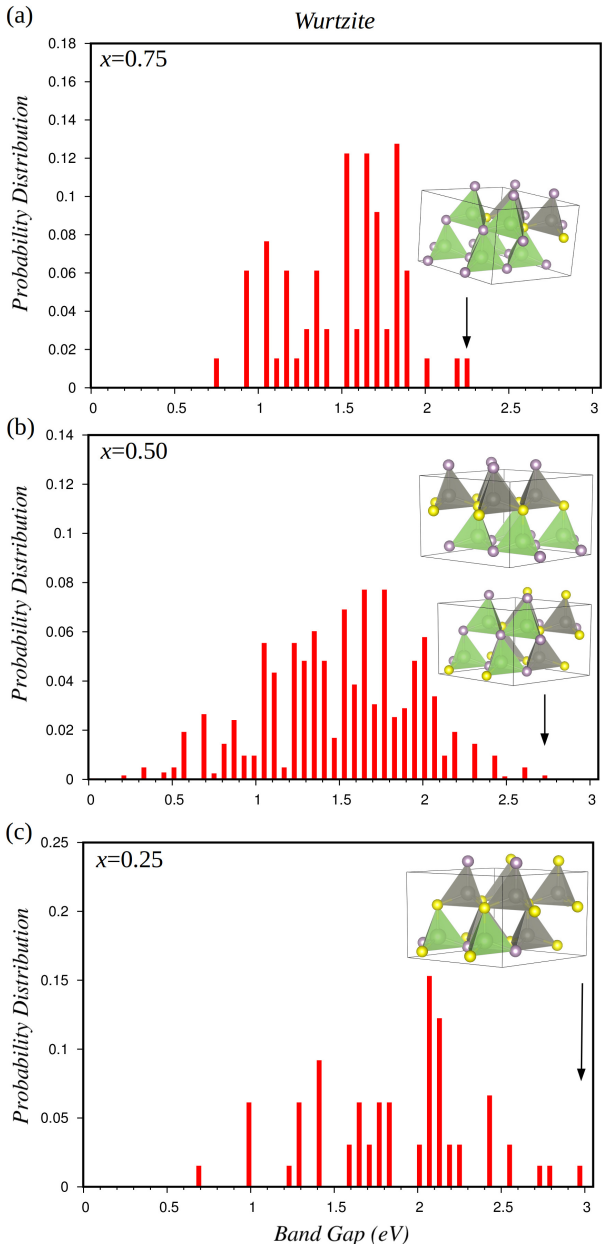

Supplementary Figure 4: Normalized E_{gap} histogram calculated in the ensemble of configurations generated for the wurtzite phase. (a) $x = 75$, (b) 50, and (c) 25% compositions. The inequivalent configurations that are most likely to occur at room temperature are sketched in each case along with the corresponding energy band gaps indicated with a black arrow; in the $x = 75$ and 25% cases the sketched configurations occur with 100% probability at $T = 300$ K, whereas in the $x = 50\%$ case the two configurations occur with $\sim 50\%$ probability. Ga and Zn atoms are represented with green and black spheres and P and S atoms with purple and yellow spheres, respectively. Energy band gaps are estimated with the exchange-correlation HSE06 hybrid functional[6].

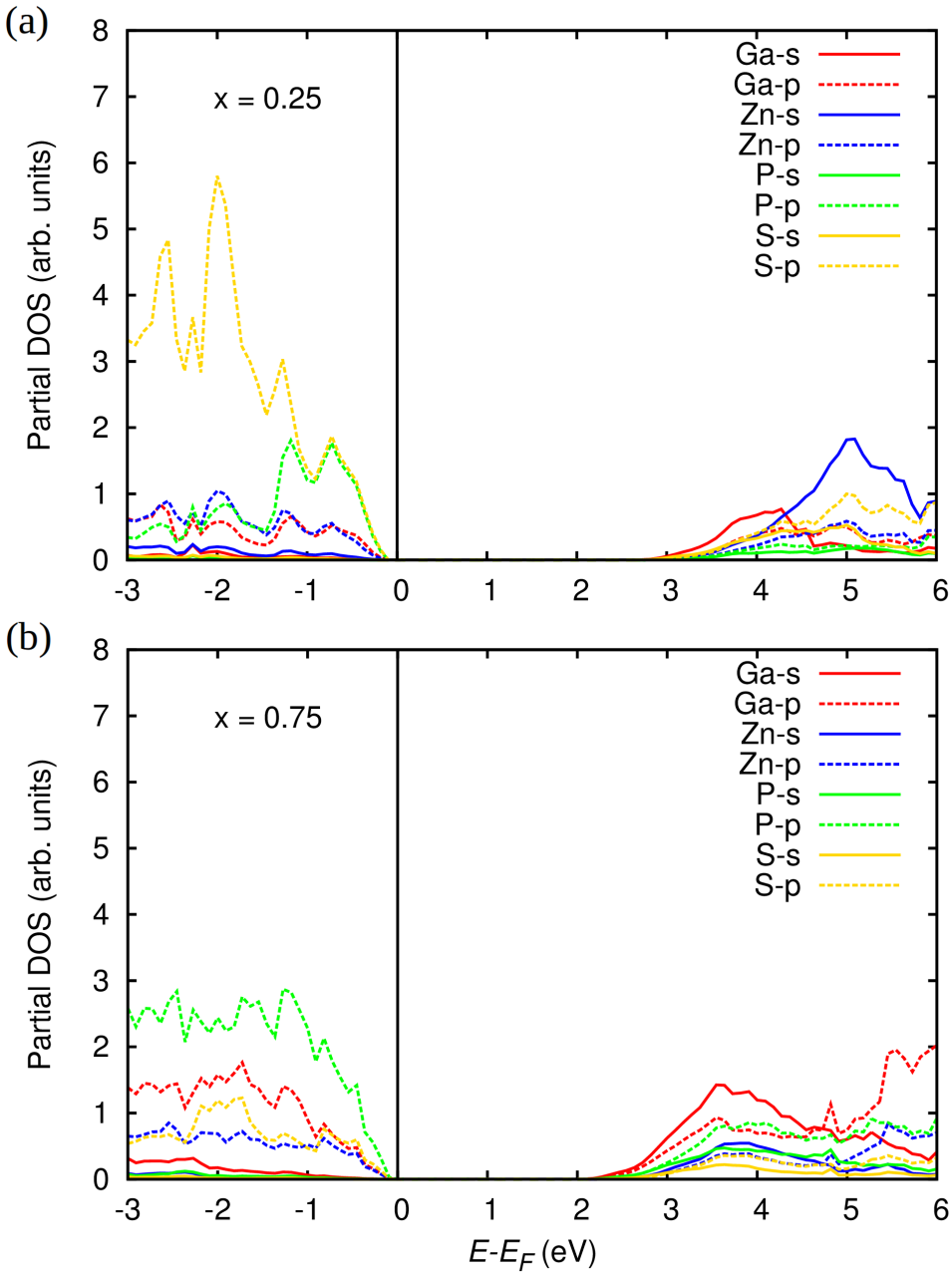

Supplementary Figure 5: Partial density of electronic states in zinc-blende $(GaP)_x(ZnS)_{1-x}$ solid solutions calculated at $x = 25$ and 75%. For clarity purposes, electronic Ga d orbitals are not represented in the figure as they are not relevant. Results are obtained with the exchange-correlation HSE06 hybrid functional[6].

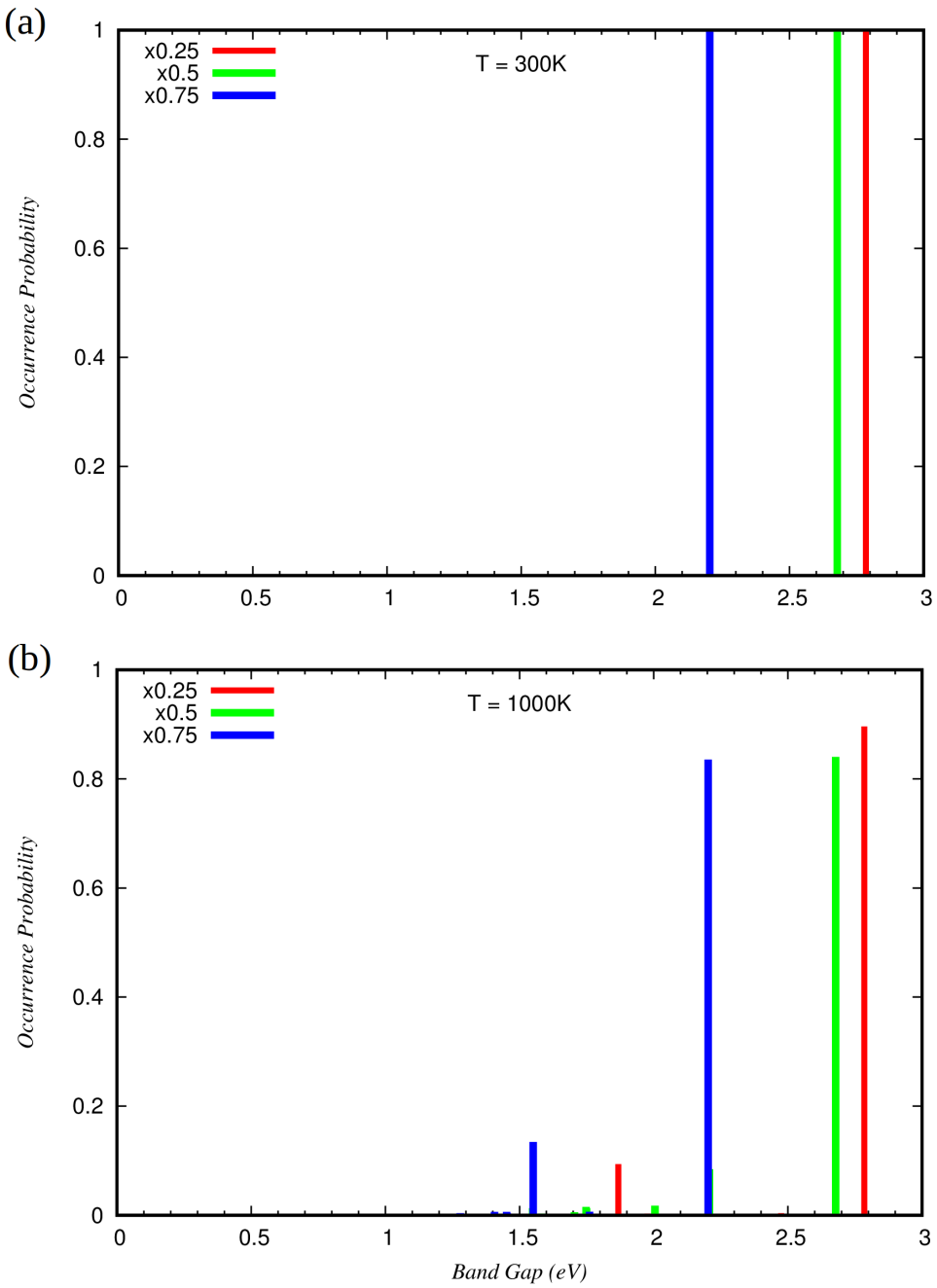

Supplementary Figure 6: Occurrence probabilities of the inequivalent configurations generated for zinc-blende $(GaP)_x(ZnS)_{1-x}$ solid solutions at room temperature and $T = 1000$ K. Compositions $x = 25$, 50, and 75% have been considered. At $T = 300$ K, we find that only the lowest-energy inequivalent configuration, which is degenerate, has an ocurrence probability different from zero. As temperature is raised, the occurrence probability of other similar inequivalent configurations start to increase.

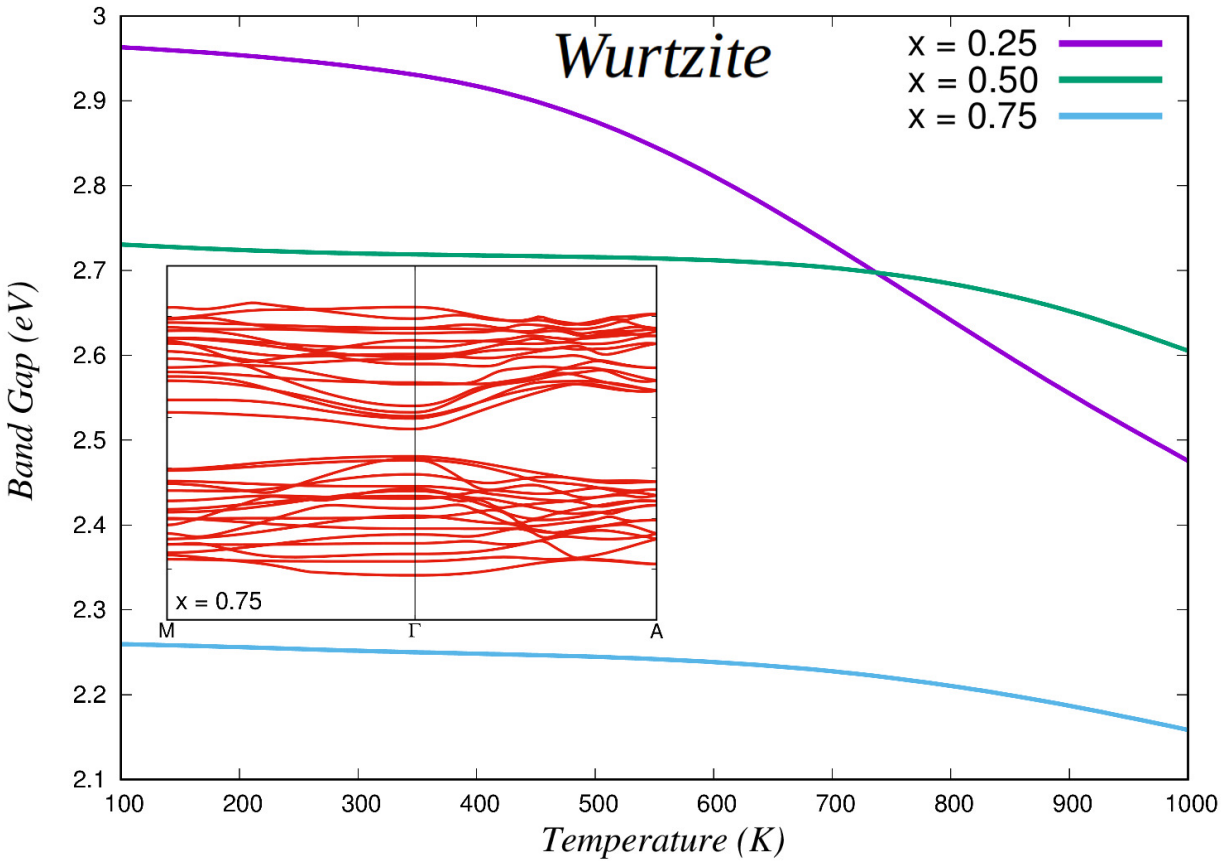

Supplementary Figure 7: Energy band gap of $(GaP)_x(ZnS)_{1-x}$ solid solutions in the wurtzite phase expressed as a function of temperature and composition. The inset shows the electronic band structure calculated in the 75% composition case, which renders a direct energy band gap at Γ (as it occurs also in the zinc-blende phase). Energy band gaps are estimated with the exchange-correlation HSE06 hybrid functional[6].

SUPPLEMENTARY REFERENCES

[1] Perdew, J. P., Burke, K. & Ernzerhof, M. Generalized gradient approximation made simple. *Phys. Rev. Lett.* **77**, 3865 (1996).

[2] Kresse, G. & Fürthmuller, J. Efficient iterative schemes for ab initio total-energy calculations using a plane-wave basis set. *Phys. Rev. B* **54**, 11169 (1996); Kresse, G. & Joubert, D. From ultrasoft pseudopotentials to the projector augmented-wave method. *Phys. Rev. B* **59**, 1758 (1999).

[3] Blöchl P. E. Projector augmented-wave method. *Phys. Rev. B* **50**, 17953 (1994).

[4] Heyd, J., Peralta, J. E., Scuseria, G. E. & Martin, R. L. Energy band gaps and lattice parameters evaluated with the Heyd-Scuseria-Ernzerhof screened hybrid functional. *J. Chem. Phys.* **123**, 174101 (2005).

[5] Hart, J. N. & Allan, N. L. GaPZnS solid solutions: Semiconductors for efficient visible light absorption and emission. *Adv. Mater.* **25**, 2989 (2013).

[6] Krukau, A. V., Vydrov, O. A., Izmaylov, A. F. & Scuseria, G. E. Influence of the exchange screening parameter on the performance of screened hybrid functionals. *J. Chem. Phys.* **125**, 224106 (2006).

[7] Kresse, G., Furthmüller, J. & Hafner, J. Ab initio force constant approach to phonon dispersion relations of diamond and graphite. *Europhys. Lett.* **32**, 729 (1995).

[8] Alfè, D. PHON: a program to calculate phonons using the small displacement method. *Comp. Phys. Commun.* **180**, 2622 (2009).

[9] Cazorla, C., Diéguez, O. & Íñiguez, J. Multiple structural transitions driven by spin-phonon couplings in a perovskite oxide. *Sci. Adv.* **3**, e1700288 (2017).

[10] Cazorla, C. & Íñiguez, J. Insights into the phase diagram of bismuth ferrite from quasiharmonic free-energy calculations. *Phys. Rev. B* **88**, 214430 (2013).

[11] Togo, A. & Tanaka, I. First principles phonon calculations in materials science. *Scr. Mater.* **108**, 1 (2015).

[12] Dovesi, R., Orlando, R., Civalleri, B., Roetti, C., Saunders, V. R. & Zicovich-Wilson, C. M. CRYSTAL: a computational tool for the ab initio study of the electronic properties of crystals. *Z. Kristallogr.* **220**, 571 (2005).

[13] Causà, M., Dovesi, R. & Roetti, C. Pseudopotential Hartree-Fock study of seventeen III-V and

IV-IV semiconductors. *Phys. Rev. B* **43**, 11937 (1991).

[14] Jaffe, J. E. & Hess, A. C. Hartree-Fock study of phase changes in ZnO at high pressure. *Phys. Rev. B* **48**, 7903 (1993).

[15] Lichanot, A., Aprà, E. & Dovesi, R. Quantum mechnical HartreeFock study of the elastic properties of Li_2S and Na_2S. *Phys. Stat. Sol. B* **177**, 157 (1993).

[16] Becke, A. D. Densityfunctional thermochemistry. III. The role of exact exchange. *J. Chem. Phys.* **98**, 5648 (1993).